THE MULTI-STEP CADIS METHOD FOR SHUTDOWN DOSE RATE CALCULATIONS AND UNCERTAINTY PROPAGATION

RADIATION TRANSPORT AND PROTECTION

KEYWORDS: *hybrid Monte Carlo/deterministic techniques, Multi-Step CADIS, shutdown dose rate*

AHMAD M. IBRAHIM,* DOUGLAS E. PEPLOW, ROBERT E. GROVE, JOSHUA L. PETERSON, and SETH R. JOHNSON

Oak Ridge National Laboratory, Reactor and Nuclear Systems Division, P.O. Box 2008, Building 5700, Oak Ridge, Tennessee 37831-6170

Received January 2, 2015
Accepted for Publication June 8, 2015
http://dx.doi.org/10.13182/NT15-1

PREPRINT

Shutdown dose rate (SDDR) analysis requires (a) a neutron transport calculation to estimate neutron flux fields, (b) an activation calculation to compute radionuclide inventories and associated photon sources, and (c) a photon transport calculation to estimate final SDDR. In some applications, accurate full-scale Monte Carlo (MC) SDDR simulations are needed for very large systems with massive amounts of shielding materials. However, these simulations are impractical because calculation of space- and energy-dependent neutron fluxes throughout the structural materials is needed to estimate distribution of radioisotopes causing the SDDR. Biasing the neutron MC calculation using an importance function is not simple because it is difficult to explicitly express the response function, which depends on subsequent computational steps. Typical SDDR calculations do not consider how uncertainties in MC neutron calculation impact SDDR uncertainty, even though MC neutron calculation uncertainties usually dominate SDDR uncertainty.

The Multi-Step Consistent Adjoint Driven Importance Sampling (MS-CADIS) hybrid MC/deterministic method was developed to speed SDDR MC neutron transport calculation using a deterministically calculated importance function representing the neutron importance to the final SDDR. Undersampling is usually inevitable in large-problem SDDR simulations because it is very difficult for the MC method to simulate particles in all space and energy elements of the neutron calculation. MS-CADIS can assess the degree of undersampling in SDDR calculations by determining the fraction of the SDDR response in the space and energy elements that did not have any scores in the MC neutron calculation. It can also provide estimates for upper and lower limits of SDDR statistical uncertainties resulting from uncertainties in MC neutron calculation.

MS-CADIS was applied to the ITER SDDR benchmark problem that resembles the configuration and geometrical arrangement of an upper port plug in ITER. Without using the hybrid MC/deterministic methods to speed MC neutron calculations, SDDR calculations were significantly undersampled for all tallies, even when MC neutron calculation computational time was 32 CPU-days. However, all SDDR tally results with MC neutron calculations of only 2 CPU-days converged with the standard Forward-Weighted CADIS (FW-CADIS) method and the MS-CADIS method. Compared to the standard FW-CADIS approach, MS-CADIS decreased the undersampling in the calculated SDDR by factors between 0.9% and 0.3% for computational times between 4 and 32 CPU-days, and it increased the computational efficiency of the SDDR neutron MC calculation by factors between 43% and 69%.

Note: Some figures in this paper may be in color only in the electronic version.

*E-mail: ibrahimam@ornl.gov

I. INTRODUCTION

Shutdown doses in fission and fusion energy systems result from decay of neutron-induced activation products in irradiated materials. Accurate assessments of the shutdown dose rate (SDDR) are crucial to support operation, maintenance, and waste disposal planning and to guide possible design changes of key components in nuclear energy systems. An SDDR calculation involves three steps:

1. a neutron transport calculation to determine the space- and energy-dependent neutron flux distributions
2. activation calculations to compute the photon source distribution
3. a photon transport calculation for estimating the final SDDR.

Even without considering the second and the third computational steps, SDDR calculations are much more challenging than one-step neutronics calculations (e.g., the calculation of the prompt dose rate during operation) because detailed space- and energy-dependent neutron fluxes are needed in the neutron transport calculation of SDDR analysis. In some applications, full-scale SDDR simulations are required for immensely large systems that involve massive amounts of shielding materials. These simulations require calculating the distribution of radioisotopes throughout the entire system. For example, SDDR assessments are required throughout the biological shield (bioshield) of the ITER experimental facility to (a) evaluate the required waiting period after the shutdown of ITER and (b) identify the locations where human accessibility should be prohibited.[1] The bioshield is a large cylindrical concrete structure (~30 m tall and 30 m in diameter) surrounding the very complex tokamak machine. Determining the effects on SDDR due to important factors such as the cross talk (interactions) between the different ports of ITER is possible only through full-scale simulations that involve all the complex inner details of the ITER tokamak machine.

Because discrete ordinates (S_N) methods provide detailed flux information, they may seem more appropriate than Monte Carlo (MC) methods for SDDR neutron transport calculations; however, the truncation errors of S_N methods can adversely affect the accuracy of SDDR predictions. Furthermore, some of the SDDR analyses involve radiation streaming through very narrow solid angles and many very complicated pathways that cannot be appropriately handled by S_N methods. The computational requirements of full-scale structured-mesh S_N simulations for very large and complicated systems such as ITER (on the order of tens of processor-years) are manageable only using world-class supercomputers.[2] Even with such expensive requirements, some important geometric features of these complex systems can never be accurately represented using structured-mesh S_N codes. Unstructured-mesh S_N simulations have been used to calculate SDDR at the interspaces of the ITER diagnostics ports. However, these calculations required limited angular discretization and the use of coarse meshes with sizes on the order of tens of centimeters in some regions because of the limited scaling capabilities (up to hundreds of processors) of the unstructured-mesh S_N codes used.[3] These coarse meshes and limited angular discretization cause severe discretization errors that can be evidenced by the appearance of negative space- and energy-dependent neutron fluxes in the S_N solutions.[4]

The rigorous two-step (R2S) computational system entails Monte Carlo neutron and photon transport calculations coupled with a comprehensive activation step using a dedicated inventory code and library.[5] Accurate full-scale R2S simulations are impractical for large, geometrically complex problems because the calculation of space- and energy-dependent neutron fluxes throughout the structural materials is difficult using the MC method. Biasing the neutron MC calculation using an importance function[6] is not straightforward because it is difficult to explicitly express the response function of the neutron calculation, which depends on the subsequent calculation steps. Moreover, typical R2S calculations do not consider the impact of uncertainties in the MC neutron calculation on SDDR uncertainty, even though these former uncertainties usually dominate the SDDR uncertainty.[7]

We developed the Multi-Step Consistent Adjoint Driven Importance Sampling (MS-CADIS) hybrid MC/deterministic method to speed up the SDDR MC neutron transport calculation using an importance function that represents the neutron importance to the final SDDR. The MS-CADIS method uses the CADIS method, which has been successfully used for more than a decade in shielding calculations,[8] to develop consistent source biasing and weight window (WW) variance-reduction parameters that efficiently modify the sampling of particles without encountering inefficiency and false convergence problems caused by the incompatibility between source and transport biasing.[9] However, because the MS-CADIS method focuses on multistep shielding calculations such as the R2S calculations of SDDR, it develops an importance function for the initial radiation transport calculation (e.g., the neutron calculations in SDDR simulations) that represents the importance of particles to the final response of the overall simulation. This paper explains the theory of the MS-CADIS method and provides some insights into the physical interpretations of the MS-CADIS adjoint neutron source and the MS-CADIS adjoint neutron flux. This paper also describes the viability and practicality of using the MS-CADIS method to assess the reliability of the SDDR MC calculations and to calculate the SDDR uncertainty resulting from uncertainties in the MC neutron calculation.

The initial MS-CADIS implementation used the Standardized Computer Analyses for Licensing Evaluation, Version 6.1 (SCALE 6.1) (Ref. 10), shielding analysis sequence Monaco with Automated Variance

PREPRINT

Reduction using Importance Calculations (MAVRIC) (Ref. 11), for the radiation transport calculations and the SCALE 6.1 Oak Ridge Isotope GENerator (ORIGEN) package[12] to complete the activation and decay calculations. In this paper, the effectiveness of the MS-CADIS method in speeding up SDDR MC calculations, in calculating SDDR uncertainty due to uncertainties of MC calculations of neutron flux distribution, and in assessing the reliability of SDDR MC calculations is demonstrated. The demonstration used an ITER benchmark problem[13] that resembles the configuration and geometrical arrangement of an upper port plug in ITER.

II. THE MS-CADIS METHOD

II.A. MS-CADIS Importance Function

Many techniques have been developed to reduce the variance or increase the efficiency of MC calculations. These modified sampling techniques alter the MC transport simulation in an attempt to sample more particles in the phase-space regions that contribute to the tally. The importance sampling technique[6] uses an importance function—the expected score to a detector from a particle at some point in phase-space—to modify the MC sampling process. The importance function $I(\vec{r},E)$ can also be viewed as the exact response of the detector due to a source represented by delta function in space $q(\vec{r},E) = \delta(\vec{r}-\vec{r}_0)\delta(E-E_0)$. Theoretically, if $I(\vec{r},E)$ is known exactly, the detector response R can be expressed as

$$R = \int_V \int_E I(\vec{r},E) q(\vec{r},E)\, dV dE \ , \qquad (1)$$

where $q(\vec{r},E)$ is the source distribution function.[a] Equation (1) represents an integral equation describing a hypothetical, absolutely efficient MC process in which each simulated particle scores the exactly correct expected value as soon as it is emitted from the source without undergoing any physical events. It is necessary to mention that finding the exact importance function is unrealistic.[6] If the exact importance function could be known, the random sampling process would not be needed because it would be easier to calculate the response using integration methods. However, over the last two decades, some hybrid MC/deterministic techniques have been very successful in dramatically increasing the efficiency of MC calculations using approximate importance functions.[8] The crux of the MS-CADIS approach is to calculate an appropriate approximation for the importance function $I(\vec{r},E)$, recognizing that even for the initial steps in multistep calculations, the response R in Eq. (1) should be the final response of the overall analysis, not the response of each step on its own.

[a]For simplicity, all the distributions were assumed to be isotropic, but the derivation can be generalized to include the angular variation in a straightforward way.

For the linear integrodifferential neutral particle transport equation, a related adjoint equation can be formulated using the identity

$$\langle \phi(\vec{r},E), q^+(\vec{r},E)\rangle = \langle \phi^+(\vec{r},E), q(\vec{r},E)\rangle \ , \qquad (2)$$

where

$\phi(\vec{r},E)$ = space- and energy-dependent particle flux

$\phi^+(\vec{r},E)$ = space- and energy-dependent adjoint flux

$q^+(\vec{r},E)$ = adjoint source space and energy distribution function

and the angle brackets $\langle\cdot\rangle$ signify integration over all energy and space. This adjoint identity is valid for an arbitrary adjoint source function.[14] However, if the adjoint source function is carefully chosen so that the left side of Eq. (2) represents the response R in Eq. (1), Eq. (2) will have the same form as Eq. (1) if the importance function $I(\vec{r},E)$ is defined as the exact solution of the adjoint transport equation with that specific choice of the adjoint source function.

The SDDR caused by decay photons is defined as

$$\text{SDDR} = \langle \sigma_d(\vec{r},E_p), \phi_p(\vec{r},E_p)\rangle \ , \qquad (3)$$

where

σ_d = flux–to–dose rate conversion factor at the position of the detector

ϕ_p = photon flux.

Using Eqs. (2) and (3) and setting the photon adjoint source equal to σ_d leads to the following relationship for the photon transport problem:

$$\text{SDDR} = \left\langle q_p^+(\vec{r},E_p), \phi_p(\vec{r},E_p)\right\rangle = \left\langle q_p(\vec{r},E_p), \phi_p^+(\vec{r},E_p)\right\rangle \ . \qquad (4)$$

Because the adjoint photon flux $\phi_p^+(\vec{r},E_p)$ in Eq. (4) expresses the final SDDR caused by a unit photon source at position $\vec{r}$ and with energy E_p, an approximate deterministic estimate of the photon adjoint flux can be used to speed up the MC photon transport calculation of an SDDR problem.

In SDDR analyses, the neutron and photon calculations are separated by an activation calculation. Finding the adjoint source of the SDDR neutron calculation is not as simple as the photon calculation because the SDDR is not directly caused by the neutrons but rather is caused by the decay photons of the neutron-activated structural materials. In the MS-CADIS method, we seek an adjoint neutron source whose inner product satisfies the following relationship for the neutron transport problem:

$$\text{SDDR} = \left\langle q_n^+(\vec{r},E_n), \phi_n(\vec{r},E_n)\right\rangle = \left\langle q_n(\vec{r},E_n), \phi_n^+(\vec{r},E_n)\right\rangle \ , \qquad (5)$$

where

PREPRINT

q_n = neutron source

ϕ_n = neutron flux

q_n^+ = neutron adjoint source

ϕ_n^+ = neutron adjoint flux.

While it may seem counterintuitive to set the *neutron* adjoint identity to be equal to a *photon* response, this leads to the development of an importance function that represents the importance of the neutrons to the SDDR. From Eqs. (4) and (5), it is clear that the MS-CADIS adjoint neutron source will satisfy the integral equation

$$\left\langle q_n^+(\vec{r},E_n),\phi_n(\vec{r},E_n)\right\rangle = \left\langle q_p(\vec{r},E_p),\phi_p^+(\vec{r},E_p)\right\rangle . \quad (6)$$

If a relationship between the photon source and the neutron flux can be determined, then an adjoint neutron source whose inner product satisfies Eq. (7) can be found.

The photon source can be calculated using a deterministic neutron transport calculation followed by an activation calculation, but finding the relationship between the photon source and the neutron flux requires considering all neutron transmutation interactions that affect the radioisotope inventory. The exact equation describing the radioisotope inventory as a function of the neutron flux is rather complicated.[15] However, a simple relationship between the photon source and the neutron flux can be derived using quantities calculated by a deterministic neutron transport calculation followed by an activation calculation.

At the end of a fixed irradiation and decay scenario, the photon source that originates from the decay of different radioisotopes can be represented by

$$q_p(\vec{r},E_p) = \sum_i m_i(\vec{r}) f_i(E_p) , \quad (7)$$

where

m_i = mass of each radioisotope i at the end of the scenario

$f_i(E_p)$ = spectrum of one mass unit of radioisotope i.

If the scenario starts from a clean inventory of stable isotopes and we assume the neutron flux during irradiation does not change due to changes in the radioisotope inventory, $m_i(\vec{r})$ can be expressed as the sum of each mass portion of radioisotope i created due to an interaction x with a stable or an activated isotope and the decay or the depletion of the result of this interaction.

By substituting Eq. (7) into Eq. (6) and changing the order of integration, it can be shown that the following adjoint source satisfies the integral relationship of Eq. (6):

$$q_n^+(\vec{r},E_n) = \sum_t \left(\int_{E_p} f_i(E_p)\phi_p^+(\vec{r},E_p)dE_p \times \sum_x m_{ix}(\vec{r}) \frac{\sigma_{xi}(E_n)}{\sigma_{xi}(\vec{r})\phi_n^t(\vec{r})} \right). \quad (8)$$

Note that the following expression was used to facilitate the derivation:

$$m_i(\vec{r}) = \sum_x m_{ix}(\vec{r}) \frac{\int_{E_n} \sigma_{xi}(E_n)\phi_n(\vec{r},E_n)dE_n}{\sigma_{xi}(\vec{r})\phi_n^t(\vec{r})} , \quad (9)$$

where

$m_{ix}(\vec{r})$ = mass at the end of the scenario of each radioisotope i that was originally created by the interaction x at $\vec{r}$

$\sigma_{xi}(E_n)$ = energy-dependent microscopic cross section of the interaction x that leads to the creation of the radioisotope i or its precursor

$\phi_n^t(\vec{r})$ = total flux at location $\vec{r}$

$\sigma_{xi}(\vec{r})$ = one-group cross section of $\sigma_{xi}(E_n)$ that uses $\phi_n(\vec{r},E_n)$ as the collapsing vector.

Equation (9) represents this mass conservation multiplied by the same interaction rate per atom in the numerator and the denominator. If the irradiation scenario starts with an initial radioisotope inventory, this initial inventory should not be considered in the masses calculated in Eq. (9) because it does not appreciably affect the space and energy distribution of the neutron adjoint source.

Determining all of the interactions that cause the creation of each radioisotope may not be simple. Isotopes produced by activation could absorb neutrons and be transmuted into other isotopes. Some activation products may decay into other activation products, increasing the amounts of the latter. Activation products with large neutron absorption cross sections can be burned out during exposure to neutrons and can change the magnitude of the neutron flux, causing nonlinearity in the neutron transport process. Not all of these factors need to be considered in calculating the neutron adjoint source of the MS-CADIS method because the importance function needed for speeding up the MC calculation does not have to use the exact adjoint solution. Additionally, the activated structural materials in fusion energy systems do not typically have very large neutron absorption cross sections that can cause either a significant change in the radioisotope inventory by irradiation of already activated materials or a significant change in the flux. For SDDR calculations in fusion energy systems, only the major interactions that lead to the creation of radioisotopes that contribute heavily to the SDDR need to be considered in determining the neutron adjoint source. The adjoint source defined by Eq. (8) can be approximated by considering

PREPRINT

only the interactions with initial stable isotopes without considering interactions with activated radioisotopes.

The MS-CADIS adjoint neutron source defined in Eq. (8) represents the SDDR resulting from the decay of radioisotopes created through irradiation by a unit neutron flux with energy E_n at location $\vec{r}$. The intuitive response function (adjoint source) for a neutron-only single-step transport problem is the sum of macroscopic cross sections of the interactions that produce radioactive isotopes. A related factor in Eq. (8), $m_{ix}(\vec{r})\dfrac{\sigma_{xi}(E_n)}{\sigma_{xi}(\vec{r})\phi_n^t(\vec{r})}$, represents the microscopic cross section of the radioisotope production reactions multiplied by the mass of each radioisotope existing at the end of the scenario and divided by the interaction rate with one atom. This is proportional to the macroscopic radioisotope production cross section weighted by the fraction of this radioisotope existing at the end of the scenario. The additional weighting function $\int_{E_p} f_i(E_p)\phi_p^+(\vec{r},E_p)dE_p$ represents the importance of each radioisotope produced in region $\vec{r}$ to the final SDDR.

The physical significance of the MS-CADIS adjoint function can be understood by considering the SDDR at the end of the irradiation and decay scenario caused by a unit neutron source at $\vec{r}_0$ and E_0, $q_{n0} = \delta(\vec{r} - \vec{r}_0)\ \delta(E - E_0)$. The photon source resulting from the irradiation of this unit neutron source can be represented as

$$q_{p_0} = \sum_i \left(f_i(E_p) \sum_x \left(m_{ix}(\vec{r}) \times \frac{\int_{E_n} \sigma_{xi}(E_n) G_n(\vec{r}_0 \to \vec{r}, E_0 \to E_n) dE_n}{\sigma_{xi}(\vec{r}) G_n^t(\vec{r}_0 \to \vec{r}, E_0)} \right) \right) , \quad (10)$$

where

$G_n(\vec{r}_0 \to \vec{r}, E_0 \to E_n)$ = Green's function neutron transport kernel

$G_n^t(\vec{r}_0 \to \vec{r}, E_0)$ = neutron transport kernel integrated over neutron energies.

By substituting Eq. (10) into Eq. (4), the SDDR caused by irradiation of this unit neutron source can be expressed by

$$\mathrm{SDDR}_0 = \sum_i \left(\iint_V \int_{E_p} f_i(E_p)\phi_p^+(\vec{r},E_p)dE_p \times \sum_x m_{ix}(\vec{r}) \frac{\int_{E_n} \sigma_{xi}(E_n) G_n(\vec{r}_0 \to \vec{r}, E_0 \to E_n) dE_n}{\sigma_{xi}(\vec{r}) G_n^t(\vec{r}_0 \to \vec{r}, E_0)} dV \right) . \quad (11)$$

To find the MS-CADIS neutron adjoint flux $\phi_{n_0}^+$ resulting from q_{n_0}, the MS-CADIS neutron adjoint source defined in Eq. (8) and the neutron flux kernel must be substituted into the neutron adjoint identity represented by the right equality of Eq. (5). It can be easily shown that the MS-CADIS adjoint neutron flux in this case will be equal to SDDR_0 in Eq. (11). Therefore, the MS-CADIS adjoint neutron flux represents the contribution of neutrons produced at $\vec{r}_0$ and E_0 to the SDDR that represents the "final" response of the multistep simulation. It is this physical interpretation that makes the MS-CADIS adjoint neutron flux well suited for use in accelerating SDDR MC neutron calculations.

II.B. Calculating SDDR Distributions Using MS-CADIS

The CADIS method is effective in speeding up the MC calculations of localized responses (e.g., flux, dose, or reaction rate at a specific location). An extension of the CADIS method, referred to as Forward-Weighted CADIS (FW-CADIS), was developed to speed up MC calculations of distributions (e.g., mesh tallies), as well as responses at multiple detectors.[16] The FW-CADIS method uses the inverse of the responses calculated from a forward deterministic calculation to weight the source of the deterministic adjoint calculation. MS-CADIS can also be used for speeding up MC calculations of SDDR distributions using mesh tallies or multiple tallies at several locations. Similar to the FW-CADIS method, the source used in the MS-CADIS photon adjoint calculation should be defined as the flux–to–dose rate conversion factors divided by a deterministic estimate of the SDDR at the location of each mesh tally element or at each point where the SDDR is calculated.

II.C. Difference Between MS-CADIS and Global MC Techniques

The use of global MC variance-reduction techniques, including FW-CADIS, was suggested for the neutron MC calculations of SDDR analyses.[17] The goal of these global MC variance-reduction techniques is to uniformly distribute the MC computational efforts throughout numerous phase-space segments to calculate many MC tallies with nearly uniform relative uncertainties. Even though SDDR analysis requires the calculation of space- and energy-dependent neutron fluxes, the goal of the analysis is the accurate assessment of the final SDDR. Global MC variance-reduction techniques will not focus MC computational efforts on calculating the production rates of radioisotopes that will ultimately contribute to the SDDR. The prohibitive computational costs of these approaches, which increase with the overall problem size and amount of shielding materials, inhibit their ability to accurately predict the SDDR in fusion energy systems using full-scale modeling of an entire fusion plant. Accurate full-scale simulations are required in the design analysis of fusion energy systems such as ITER to determine the effects of important factors such as the cross talk between the different ports on the SDDR behind the ports.[18] The full-scale calculation of the SDDR inside the ITER

PREPRINT

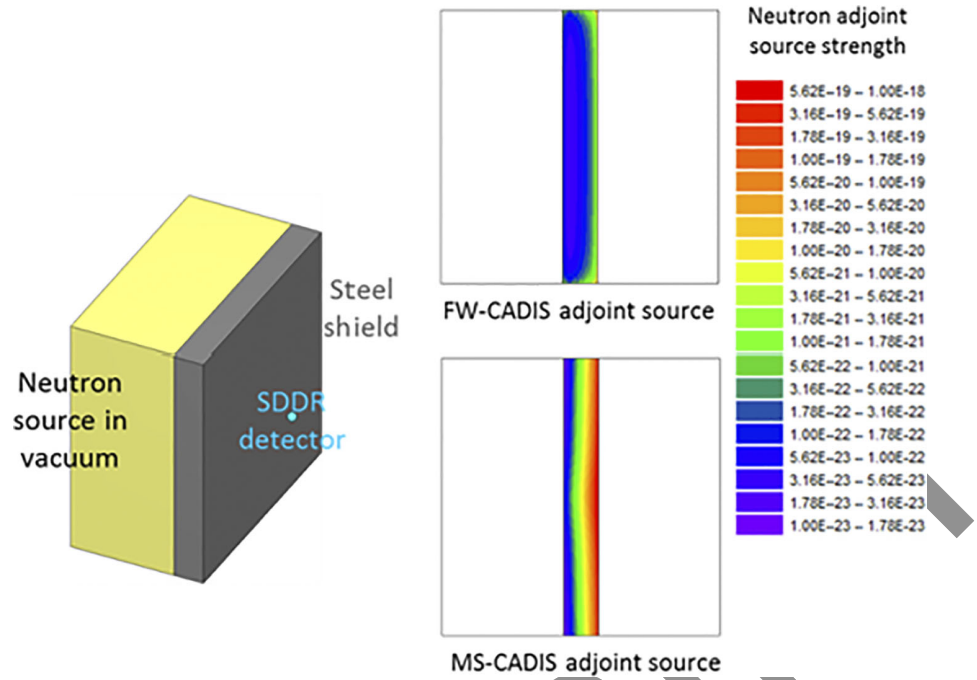

Fig. 1. FW-CADIS and MS-CADIS adjoint sources.

bioshield will require calculating the neutron fluxes in $\sim 3.8 \times 10^{10}$ space-energy mesh elements for cubic mesh elements with a side length of 5 cm and 175 energy bins.[b] Even with the unrealistic assumption of using absolutely accurate neutron fluxes for applying global MC variance-reduction techniques, the computational cost of an MC calculation with nonzero MC scoring in all of these space-energy elements will exceed tens of CPU-years. Contrary to the global MC approach, the MS-CADIS method uses a function that represents the importance of the neutrons to the final SDDR or to the final SDDR distribution. This ensures that the computational effort in the MC neutron calculation is focused on the most important parts of the problem, enabling accurate, large-scale three-dimensional MC analyses of SDDR.

To illustrate the difference between the MS-CADIS method and global MC methods, the neutron adjoint sources created using the FW-CADIS and MS-CADIS methods for a simple slab shield problem are shown in Fig. 1. The maximum adjoint source strength of the FW-CADIS method is at the far corners of the detector side of the steel shield where the forward flux is minimal, while the maximum MS-CADIS adjoint source strength is at the center of the detector side of the steel shield because the activated radioisotopes in this region have the greatest contribution to the SDDR at the detector.

[b]The fine multigroup Fusion Evaluated Nuclear Data Library[19] (FENDL) 2.1 that is typically used in fusion applications has 175 neutron energy groups.

II.D. MS-CADIS Implementation

The R2S computational system is based on coupling the activation and MC transport codes and libraries to provide the neutron fluxes calculated from the MC neutron calculation to the activation step and to use the decay photon source in the photon MC calculation. In addition to these calculations, MS-CADIS requires performing the following steps:

step 1: a forward deterministic neutron transport calculation to estimate $\sigma_{xi}(\vec{r})$ and $\phi_n^t(\vec{r})$

step 2: activation calculations for each isotope at each element of the deterministic mesh to estimate $m_{ix}(\vec{r})$

step 3: an adjoint deterministic photon transport calculation using an adjoint source equal to the flux–to–dose rate conversion factors at the position of the SDDR detector

step 4: an adjoint deterministic neutron transport calculation with an adjoint source calculated from Eq. (8).

Using the CADIS method, the deterministically calculated adjoint neutron and photon fluxes can be used to calculate the source biasing and WW parameters to speed up the R2S neutron and photon MC calculations.

Assuming all of the important radioisotope-producing neutron interactions were accounted for in Eq. (8), the quantity $\frac{m_{ix}(\vec{r})}{\sigma_{xi}(\vec{r})\phi_n^t(\vec{r})}$, which primarily depends on the mass of the initial stable isotope and on the irradiation and

PREPRINT

decay scenario, should not significantly change with the magnitude and the energy distribution of the neutron flux. The activation calculations in step 2 need to be repeated only a few times with different neutron energy distributions to calculate an appropriate value for $\frac{m_{ix}(\vec{r})}{\sigma_{xi}(\vec{r})\phi_n^t(\vec{r})}$. This value can be used for calculating the adjoint neutron source at any location $\vec{r}$.

II.E. Assessment of the Degree of Undersampling in MC SDDR Calculations

As noted in Sec. II.C, MC calculations of energy-dependent neutron fluxes throughout an entire geometry are very difficult to complete for large and complicated problems. The inability of the MC method to calculate nonzero MC fluxes in all space-energy elements can cause significant undersampling in SDDR calculations. However, not all of these elements are important to the SDDR calculation. Elements with energies at which the cross sections of the radioisotope-producing neutron transmutation reactions are very small, as well as elements that are very far from the locations at which the SDDR is calculated, will have only negligibly small contributions to the SDDR at these locations. An assessment of the importance of the elements with nonzero MC scoring (a calculated MC result) is indispensable for evaluating the reliability of MC SDDR calculations.

A deterministic approximation for the contribution of each space-energy element to the SDDR at a certain location can be estimated by multiplying the MS-CADIS adjoint source strength at that element by the deterministic neutron (forward) flux estimate at this element. The fraction of nonzero-scoring elements important to the SDDR can be determined by adding these SDDR contributions in all the nonzero-scoring elements and dividing this sum by the deterministic estimate of the total SDDR. This deterministic approximation of the fraction of the SDDR response that exists in nonzero-scoring space-energy elements can be used as the reliability metric to determine the degree of undersampling in SDDR calculations. This reliability metric *RM* can be expressed as

$$RM = \sum_{ijkg} \frac{\xi_{n_{ijkg}} \phi_{n_{ijkg}} q^+_{n_{ijkg}}}{\phi_{n_{ijkg}} q^+_{n_{ijkg}}} \ , \tag{12}$$

where

$\phi_{n_{ijkg}}$ = neutron flux at the space-energy elements *ijkg*

$q^+_{n_{ijkg}}$ = neutron adjoint flux that is defined by Eq. (8) at the same element

$\xi_{n_{ijkg}}$ = factor that is either one for nonzero-scoring elements or zero for zero-scoring elements.

It is necessary to mention that the calculation of this factor requires that the deterministic and the neutron MC calculations use the same mesh. Interpolation techniques will be needed if the deterministic calculations use a different mesh than the one used for the neutron MC mesh tally. If the calculation involves more than one SDDR tally, each SDDR tally can have its own *RM*. Each *RM* will require a separate neutron adjoint source function, q_n^+, representing the SDDR at the location of this tally due to a unit neutron source at each space-energy element. For each SDDR tally, a separate photon adjoint calculation has to be performed using a photon adjoint source defined at the tally location. By substituting the photon adjoint flux of each calculation in Eq. (8), q_n^+ can be calculated for each tally.

II.F. Uncertainty Propagation Using the MS-CADIS Method

A method that uses a single deterministic photon adjoint calculation has been developed to estimate the lower bound of the statistical SDDR uncertainty resulting from statistical uncertainties in the photon source.[20] This method cannot be used directly in R2S calculations without propagating the uncertainties in the neutron fluxes into the activation calculations. However, using quantities generated during the implementation of the MS-CADIS method, one can derive an extension of this method to calculate the SDDR uncertainties resulting from stochastic uncertainties in the neutron fluxes.

In the R2S computational system, the total SDDR uncertainty is expressed as

$$\sigma^2_{\text{SDDR}} = \sigma_n^2 + \sigma_p^2 \ . \tag{13}$$

The standard deviation σ_p, which reflects the stochastic uncertainty of the MC photon transport simulation, can be calculated during the MC photon transport calculation. However, the SDDR uncertainty due to the neutron MC calculation, σ_n, cannot be easily calculated. If the neutron fluxes are calculated using a mesh tally, the total SDDR uncertainty due to the uncertainty in the neutron MC calculation can be expressed as

$$\sigma_n^2 = \sum_{ijkg} \left(\frac{\partial \text{SDDR}}{\partial \phi_{n_{ijkg}}}\right)^2 \sigma^2_{ijkg} + 2\sum_{ijkg<l} \left(\frac{\partial \text{SDDR}}{\partial \phi_{n_{ijkg}}}\right) \times \left(\frac{\partial \text{SDDR}}{\partial \phi_{n_l}}\right) \rho_{ijkg,l} \sigma_{ijkg} \sigma_l \ , \tag{14}$$

where $\rho_{ijkg,l}$ is the correlation coefficient expressing the correlation of fluxes at the space-energy elements *ijkg* and *l*. Space-energy elements farther away from each other are most likely uncorrelated ($\rho_{ijkg,l} = 0$). Reference 20 states that it is unlikely that any pair of elements has any degree of anticorrelation ($\rho_{ijkg,l} < 0$). This is especially true in the fixed-source shielding calculations of fusion energy systems. A lower bound of σ_n can be found by setting $\rho_{ijkg,l} = 0$ for all space-energy elements in Eq. (14):

PREPRINT

$$\sigma_n^2 = \sum_{ijkg} \left(\frac{\partial \mathrm{SDDR}}{\partial \phi_{n_{ijkg}}} \right)^2 \sigma_{ijkg}^2 \ , \tag{15}$$

and an upper bound can be found by setting $\rho_{ijkg,l} = 1$:

$$\sigma_n = \sum_{ijkg} \frac{\partial \mathrm{SDDR}}{\partial \phi_{n_{ijkg}}} \cdot \sigma_{ijkg} \ , \tag{16}$$

which assumes perfect linear correlation between all space-energy elements.

The first equality in Eq. (5) can be approximately expressed in a discretized form as

$$\mathrm{SDDR} = \sum_{ijkg} \phi_{n_{ijkg}} q_{n_{ijkg}}^{+} \ , \tag{17}$$

where the MS-CADIS adjoint neutron source $q_{n_{ijkg}}^{+}$ represents the SDDR due to the neutron flux at space-energy element *ijkg*. By differentiating this discretized form, the lower bound in Eq. (15) can be expressed as

$$\sigma_{n_{lower}}^2 = \sum_{ijkg} \left(q_{n_{ijkg}}^{+} \right)^2 \sigma_{ijkg}^2 \ , \tag{18}$$

and the upper bound in Eq. (16) can be expressed as

$$\sigma_{n_{upper}} = \sum_{ijkg} q_{n_{ijkg}}^{+} \cdot \sigma_{ijkg} \ . \tag{19}$$

Assuming the deterministic calculations use the same mesh of the tallies of the MC neutron calculation, Eqs. (18) and (19) can be used to estimate the statistical uncertainties in the SDDR due to the statistical uncertainty in the neutron MC calculation. However, Eqs. (18) and (19) represent only lower and upper bounds for the real uncertainty that lies between these limits. In order to provide more accurate estimates of the contribution of the neutron flux uncertainties to the overall SDDR uncertainties, future work will explore the degree to which the neutron flux space-energy elements are correlated.

It is necessary to mention that these limits of statistical uncertainties will be valid only if the statistical uncertainties in the neutron MC calculation σ_{ijkg} are known for every space-energy element. The statistical uncertainties of zero-scoring mesh tally elements are not defined. Because SDDR MC neutron calculations often have zero-scoring mesh tally elements, the calculation of the uncertainties' limits using Eqs. (18) and (19) should be limited only to cases where the undersampling due to the zero-scoring elements is very small. For these calculations, the degree of undersampling can be assessed using the reliability metric defined in Eq. (12).

This method is not directly applicable for more than one SDDR detector because the calculation of the uncertainty of each SDDR detector will require a separate adjoint source function q_n^{+}. Each q_n^{+} can be calculated according to Eq. (8) using a photon adjoint flux $\left(\phi_p^{+}\right)$ calculated with a photon adjoint source defined at each detector location.

III. ITER BENCHMARK PROBLEM

The preliminary demonstration of the MS-CADIS problem used the ITER benchmark problem.[13] This problem was used to demonstrate the effectiveness of the MS-CADIS problem in (a) speeding up the MC SDDR calculations, (b) assessing the degree of undersampling in MC SDDR calculations due to the inability of the neutron MC calculations to score in all space-energy elements, and (c) calculating the SDDR uncertainties due to MC uncertainties in calculating the neutron fluxes. The model, which resembles the configuration and geometrical arrangement of an upper port plug in ITER, is shown in Fig. 2. It consists of a 700-cm-long cylinder with a 100-cm radius. It has a central straight-streaming path with a radius of 7.5 cm. A 48-cm-radius stainless steel/water (80%/20%) shielding zone with a length of 210 cm surrounds the central streaming path. The outer shielding zone is made of 100% stainless steel. It has a rear 15-cm-thick stainless steel plate. A 2-cm straight gap between the outer and inner shielding zones extends all the way through the model. A large 325-cm-long cavity runs between the back of the stainless steel/water shield and the rear plate. A 14.1-MeV isotropic neutron source with a thickness of 1 cm is represented by a disk region placed at a distance of 10 cm from the front edge. The SDDR is calculated using four tallies representing four concentric annular disks, each 10 cm thick. All the disks are placed in air at a distance of 30 cm from the rear plate. The inner-outer radii of the disks are 0 to 15 cm, 15 to 30 cm, 30 to 45 cm, and 45 to 60 cm. Figure 2 also shows the SDDR tally cells.

The source strength and irradiation history used for the ITER benchmark problem are shown in Table I (Ref. 21). The maximum source strength, 2.8×10^{19} n/s, is calculated by scaling the neutron production rate corresponding to the operation of ITER at 700 MW by the actual loading received by the upper port plug.[13] The SDDR was calculated at the four tallies following 10^6 s of decay after the last power step in the irradiation scenario.

III.A. Methodology

The SCALE 6.1 (Ref. 10) shielding analysis sequence MAVRIC (Ref. 11) was used for the neutron and photon transport calculations, and the ORIGEN code system[12] was used for the activation and decay calculations in this analysis. MAVRIC uses the discrete ordinates structured-mesh code Denovo[22] for the deterministic calculations

PREPRINT

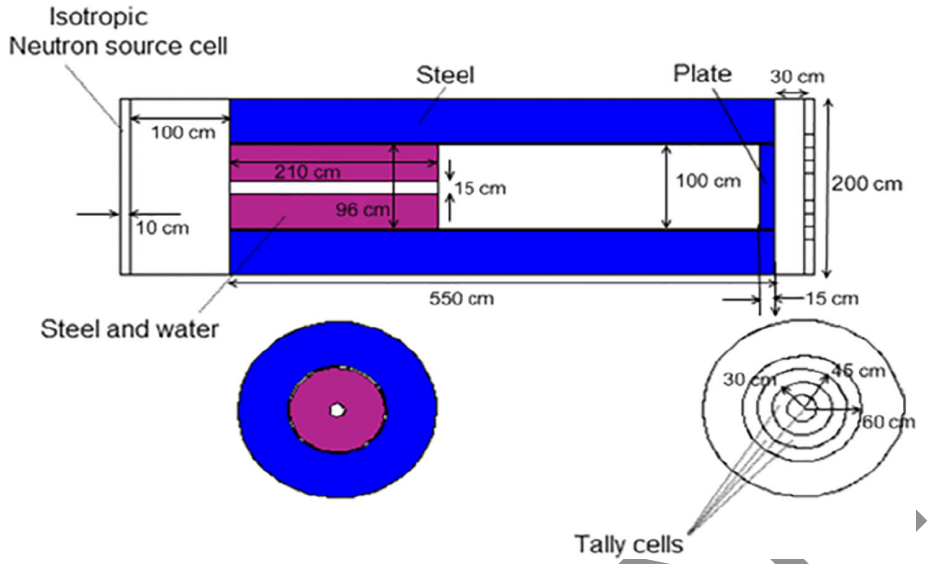

Fig. 2. ITER benchmark problem geometry and SDDR tallies.

TABLE I

Irradiation Scenario for the ITER SDDR Benchmark Problem

Source Strength (n/s)	Duration	Number of Pulses
1.0714×10^{17}	2 yr	1
8.25×10^{17}	10 yr	1
0	0.667 yr	1
1.6607×10^{18}	1.33 yr	1
0	3920 s	17
2.0×10^{19}	400 s	17
0	3920 s	4
2.8×10^{19}	400 s	4

and the multigroup MC code Monaco for the MC calculations.[11] A 200-neutron-group evaluated nuclear data file (ENDF)/B-VII data library was used for the neutron Monaco calculations, a 27-neutron-group ENDF/B-VII data library was used for the Denovo neutron calculations, and a 19-photon-group ENDF/B-VII library was used for both the Monaco and the Denovo photon transport calculations. The ORIGEN calculations used the ENDF/B-VII decay data and 200-group ORIGEN neutron cross sections based on the Joint Evaluated Fission and Fusion File (JEFF)-3.0 special-purpose activation files.

The semiautomated coupling between Monaco and Denovo on one side and ORIGEN on the other side were implemented using Python scripts. With a total of about 250 000 mesh elements, the element sizes varied between 1.5 and 5 cm in the radial directions (x and y) and between 5 and 10 cm in the axial direction (z). In each mesh element, the material used for the Denovo and the ORIGEN calculations was set to be the material present at the center of the element in the Monaco model.

The SDDR calculations were performed using three approaches. The first approach used analog Monaco neutron calculations, the second used the standard FW-CADIS method to accelerate the Monaco neutron calculations, and the third used the MS-CADIS method. All the calculations used the same running time (1 h) for the Monaco photon calculations and used the same photon importance map (WWs) based on the CADIS method. The CADIS adjoint photon source was defined as a rectangular parallelepiped surrounding the four tallies. The side length of the CADIS adjoint photon source was 120 cm, and the height was 10 cm. The only difference between the three approaches was the method used to accelerate the Monaco neutron calculation. The use of FW-CADIS as a reference in this analysis provides a reasonable efficiency comparison with respect to other global MC methods because it has been demonstrated that methods such as FW-CADIS that use both forward and adjoint estimates are more efficient in calculating more uniform relative uncertainties across a global mesh tally than other global MC methods that use only forward estimates.[23]

III.B. SDDR Tallies

To assess the ability of each approach to reliably calculate SDDR values, the time of the Monaco neutron calculations was varied, and the SDDR was computed at the four tally cells using each approach. Other than using different neutron fluxes from the different Monaco calculations, the parameters of the activation and the photon transport calculations did not change in this

PREPRINT

analysis. Figure 3 shows the SDDR values at the four tallies as a function of the running time of the Monaco neutron calculation. It is worth mentioning that the absolute values of the SDDR tallies, which depend on the mesh and the nuclear data libraries used in the analysis, were not compared to the published results of the ITER benchmark problem. However, this work is still valuable in assessing the effectiveness of each approach because the same mesh and the same nuclear data libraries were used in all the calculations of the three different approaches.

For each approach individually, the differences between the maximum and the minimum SDDRs did not exceed 12% after 2 days of running time for the neutron Monaco calculations. However, SDDRs of the analog cases were clearly undersampled, even after 32 days of running time, for the neutron Monaco calculation.

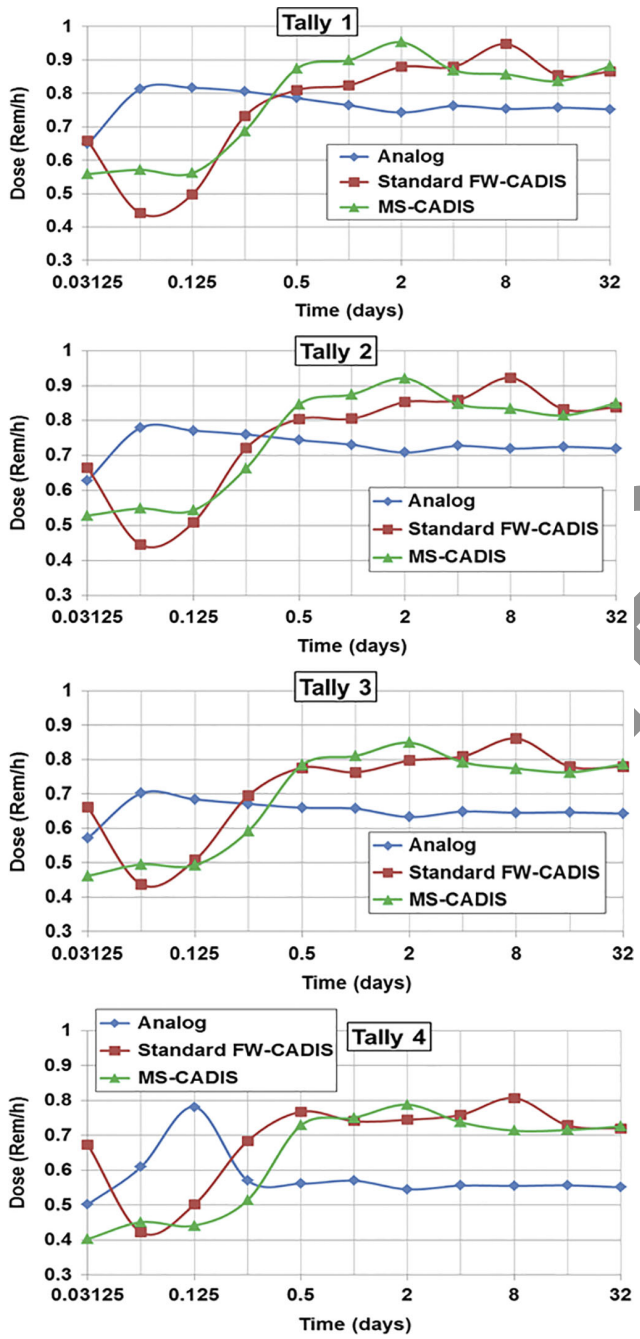

Fig. 3. SDDR estimates at the four tallies as a function of time of Monaco neutron calculations.

III.C. Degree of Undersampling

To calculate the energy-dependent neutron fluxes throughout the problem geometry, the Monaco neutron calculation used a mesh tally with 4.844×10^7 space-energy elements. In the Monaco neutron simulations, not all the space-energy tally elements received scores. In fact, the maximum fraction of the elements with nonzero MC scoring, which indicates calculating a tally result in those elements, was only 50.5% for all the Monaco neutron calculations. The nonzero fractions of space-energy elements are shown in Fig. 4 for the Monaco neutron calculations with running times >4 days. The fractions of the SDDR response that exist in nonzero-scoring elements are also shown in Fig. 4. The latter response fractions represent the reliability metrics, *RM*s, that were calculated using Eq. (12).

For all the analog cases, the fractions of nonzero-scoring elements were $<35\%$, and the fractions of the responses in nonzero-scoring elements were $<60\%$. The

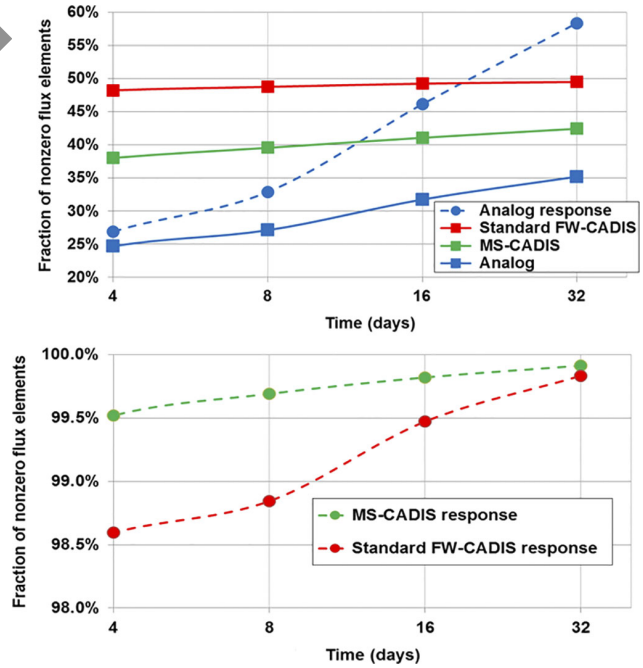

Fig. 4. Fractions of nonzero-scoring space-energy elements and fractions of SDDR responses in nonzero-scoring space-energy elements in the Monaco neutron calculations.

PRINT

fraction of nonzero-scoring elements was ~15% to 20% less with the MS-CADIS approach than with the standard FW-CADIS approach. However, the response fraction in the nonzero-scoring elements was greater by a factor of between 0.3% and 0.9% with the MS-CADIS approach. Even though the MS-CADIS method had fewer space and energy elements with nonzero scoring than the FW-CADIS method, the undersampling in the SDDR is lower with the MS-CADIS method than with the FW-CADIS method because the MS-CADIS method focuses the MC computational efforts to increase the simulated neutron population in the energy and space elements of higher importance to the final SDDR.

III.D. Uncertainty and Figure of Merit

For all the cases in which the uncertainties in the SDDR with the different approaches were compared, the relative uncertainties in the photon Monaco calculations did not exceed 1%. These uncertainties were not included in the total SDDR uncertainties because the latter were dominated by the uncertainties in the neutron Monaco calculations. Figure 5 shows the upper and lower limits of the uncertainties in the SDDR calculations for both the standard FW-CADIS and the MS-CADIS approaches.

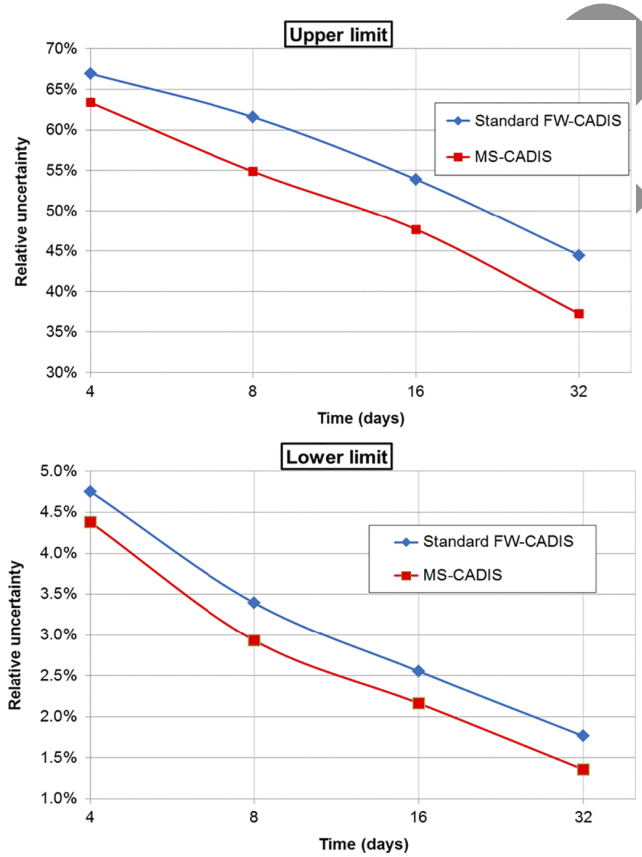

Fig. 5. Upper and lower limits of relative uncertainties in SDDR calculations.

To determine these upper and lower limits, Eqs. (18) and (19) were used to propagate the uncertainties in the neutron fluxes to the uncertainties in SDDR. The upper limit assumes a perfect linear correlation between the space and energy mesh tally elements, and the lower limit assumes no correlation between the mesh elements. For the four SDDR tallies in each calculation, only one upper limit and one lower limit for the uncertainties were calculated in this analysis. This uncertainty estimate represents the SDDR uncertainty at a detector enclosing all of the tally regions (the CADIS adjoint photon source) due to the uncertainties in the neutron Monaco calculations.

Because the estimates of uncertainties are meaningless for undersampled MC simulations, the relative uncertainties were not calculated for the analog cases or for the FW-CADIS and MS-CADIS cases with run times of <2 days for the Monaco neutron calculations. For a Monaco neutron calculation that ran for 32 days, in which the response fraction in the nonzero-scoring elements was $>99.5\%$ for both the FW-CADIS and MS-CADIS cases, the upper limit of the uncertainty was 16% less with the MS-CADIS method than with the FW-CADIS method, and the lower limit was 23% less. These limits correspond to the increases in the MC figure of merit of between 43% and 69% if the CPU times of the activation calculations and the photon transport calculations are disregarded. The MS-CADIS approach was previously shown to enhance the efficiency of an SDDR calculation by a factor of 500 compared to the standard FW-CADIS approach.[24] However, the standard FW-CADIS approach, which tends to spend more computational effort in simulating particles in the low-flux regions, is well-suited specifically for the simplified example problem in this study because the tallies were located at the regions of the lowest flux values. Additionally, the cross sections of the transmutation reactions with the highest contribution to SDDR—namely, ^{59}Co (n,γ) ^{60}Co, ^{181}Ta (n,γ) ^{182}Ta, and ^{58}Fe (n,γ) ^{59}Fe—are highest at low energies, where the neutron flux values are the lowest.

IV. CONCLUSION

The MS-CADIS method was developed to speed up SDDR MC calculations. The MS-CADIS adjoint neutron source represents the SDDR resulting from decay of the radioisotopes created through irradiation by a unit neutron flux at a certain phase-space location. The MS-CADIS adjoint neutron flux represents the contribution of neutrons produced at a certain phase-space location relative to the final. Therefore, this adjoint neutron flux is well suited to speed up SDDR MC neutron calculations using the CADIS methodology. The MS-CADIS adjoint neutron source can also be used to assess the degree of undersampling in SDDR calculations due to the inability of the MC method of simulating particles in all the space

DRAFT

and energy elements of the tallies of the MC neutron calculation as well as to determine SDDR uncertainties due to uncertainties in the neutron fluxes of the neutron MC calculation.

The application of the MS-CADIS method to SDDR calculations in fusion energy systems was tested using the ITER benchmark problem. Compared to the standard FW-CADIS method, the increase in the efficiency of the SDDR neutron MC calculation due to the use of the MS-CADIS method was between 43% and 69%. The MS-CADIS method also increases the fraction of nonzero-scoring mesh tally elements in the space-energy regions of high importance to the final SDDR. It is worth mentioning that the simplified problem used in this analysis does not replicate the conditions of the large-scale problems that motivated the development of the MS-CADIS method. Important factors such as the cross talk between the different ports in a fusion energy system cannot be quantified by the analysis of such a small problem. However, implementation of the MS-CADIS method in the SCALE and the Automated Deterministic Variance Reduction Generator[25] (ADVANTG) code systems and the demonstration using full-scale models of the ITER tokamak system are currently under way.

ACKNOWLEDGMENTS

Oak Ridge National Laboratory is managed by UT-Battelle, LLC, under contract DE-AC05-00OR22725 with the U.S. Department of Energy.

REFERENCES

1. H. IIDA et al., "Radiation Shielding for ITER to Allow for Hands-On Maintenance Inside the Cryostat," *J. Nucl. Sci. Technol.*, **37**, *Suppl. 1*, 235 (2000); http://dx.doi.org/10.1080/00223131.2000.10874882.

2. A. IBRAHIM et al., "Assessment of Fusion Facility Dose Rate Map Using Mesh Adaptivity Enhancements of Hybrid Monte Carlo/Deterministic Techniques," *Fusion Eng. Des*, **89**, 1875 (2014); http://dx.doi.org/10.1016/j.fusengdes.2014.02.046.

3. M. YOUSSEF and R. FEDER, "Summary of the Up-to-Date 3-D Nuclear Analyses of ITER Diagnostics Generic Equatorial Port Plug (GEPP) Performed with the Attila Design Code," *Fusion Sci. Technol.*, **64**, 571 (2013); http://dx.doi.org/10.13182/FST64-571.

4. R. PAMPIN et al., "Radiation Transport Analyses for Design Optimisation of the ITER Core [Light Detection and Ranging] LIDAR Diagnostic," *Fusion Sci. Technol.*, **56**, 751 (2009); http://dx.doi.org/10.13182/FST56-751.

5. Y. CHEN and U. FISCHER, "Rigorous MCNP Based Shutdown Dose Rate Calculations: Computational Scheme, Verification Calculations and Application to ITER," *Fusion Eng. Des.*, **63**, 107 (2002); http://dx.doi.org/10.1016/S0920-3796(02)00144-8.

6. G. GOERTZEL and K. KALOS, "Monte Carlo Methods in Transport Problems," *Prog. Nucl. Energy*, **2**, 315 (1958).

7. R. PAMPIN et al., "Status of Novel Tools for Estimation of Activation Dose," *Fusion Eng. Des.*, **85**, 2080 (2010); http://dx.doi.org/10.1016/j.fusengdes.2010.08.002.

8. J. C. WAGNER et al., "Review of Hybrid (Deterministic/Monte Carlo) Radiation Transport Methods, Codes, and Applications at Oak Ridge National Laboratory," *Prog. Nucl. Sci. Technol.*, **2**, 808 (2011).

9. J. C. WAGNER and A. HAGHIGHAT, "Automated Variance Reduction of Monte Carlo Shielding Calculations Using the Discrete Ordinates Adjoint Function," *Nucl. Sci. Eng.*, **128**, 186 (1998); http://dx.doi.org/10.13182/NSE98-2.

10. S. M. BOWMAN, "SCALE 6: Comprehensive Nuclear Safety Analysis Code System," *Nucl. Technol.*, **174**, 126 (2011); http://dx.doi.org/10.13182/NT10-163.

11. D. E. PEPLOW, "Monte Carlo Shielding Analysis Capabilities with MAVRIC," *Nucl. Technol.*, **174**, 289 (2011); http://dx.doi.org/10.13182/NT174-289.

12. I. C. GAULD et al., "Isotopic Depletion and Decay Methods and Analysis Capabilities in SCALE," *Nucl. Technol.*, **174**, 169 (2011); http://dx.doi.org/10.13182/NT11-3.

13. M. LOUGHLIN, "Conclusions of Shutdown Dose Rate Benchmark Study," *Proc. 6th ITER Neutronics Mtg.*, Hefei, China, June 17–24, 2011.

14. E. E. LEWIS and W. F. MILLER, JR., *Computational Methods of Neutron Transport*, American Nuclear Society, La Grange Park, Illinois (1993).

15. D. VONDY, "Development of General Method of Explicit Solution to the Nuclide Chain Equations for Digital Machine Calculations," ORNL-TM-361, Oak Ridge National Laboratory (1962).

16. J. C. WAGNER, D. E. PEPLOW, and S. W. MOSHER, "FW-CADIS Method for Global and Regional Variance Reduction of Monte Carlo Radiation Transport Calculations," *Nucl. Sci. Eng.*, **176**, 37 (2014); http://dx.doi.org/10.13182/NSE12-33.

17. A. DAVIS and A. TURNER, "Application of Novel Global Variance Reduction Methods of Fusion Radiation Transport Problems," *Proc. 2011 Int. Conf. Advances in Mathematics, Computational Methods, and Reactor Physics,* Rio de Janeiro, Brazil, May 8–12, 2011, p. 8, American Nuclear Society (2011).

18. R. PAMPIN et al., "Investigation of Radiation Cross-Talk Effects on Biological Dose Rates in Maintenance Areas Inside the ITER Tokamak," *Proc. 18th Topl. Mtg. Radiation Protection and Shielding Division*, Knoxville, Tennessee, September 14–18, 2014, American Nuclear Society (2014).

19. D. L. ALDAMA and A. TRKOV, "FENDL2.1, Update of an Evaluated Nuclear Data Library for Fusion Applications," International Atomic Energy Agency, International Nuclear Data Center, Nuclear Data Services, p. 467 (2004).

20. D. PEPLOW et al., "Propagation of Uncertainty from a Source Computed with Monte Carlo," *Trans. Am. Nucl. Soc.*, **108**, 643 (2013).

PREPRINT

21. M. LOUGHLIN and N. TAYLOR, "Recommended Plasma Scenarios for Activation Calculations," ITER_D_2V3V8G v 1.0, ITER Document Management System (2009).

22. T. M. EVANS et al., "Denovo: A New Three-Dimensional Parallel Discrete Ordinates Code in SCALE," *Nucl. Technol.*, **171**, 171 (2010); http://dx.doi.org/10.13182/NT10-5.

23. D. PEPLOW, "Comparison of Hybrid Methods for Global Variance Reduction in Shielding Calculations," *Proc. 2013 Int. Conf. Advances in Mathematics, Computational Methods, and Reactor Physics,* Sun Valley, Idaho, May 5–9, 2013, p. 231, American Nuclear Society (2013).

24. A. IBRAHIM et al., "Novel Hybrid Monte Carlo/Deterministic Technique for Shutdown Dose Rate Analyses," *Fusion Eng. Des.*, **89**, 1933 (2014); http://dx.doi.org/10.1016/j.fusengdes.2014.03.014.

25. S. W. MOSHER et al., "ADVANTG—An Automated Variance Reduction Parameter Generator," ORNL/TM-2103/416, Oak Ridge National Laboratory (2013).

PREPRINT